

SUPPLEMENTARY INFORMATION

Understanding Anharmonic Effects on Hydrogen Desorption Characteristics of Mg_nH_{2n} Nanoclusters by ab initio trained Deep Neural Network

Andrea Pedrielli^{a,b}, Paolo E. Trevisanutto^c, Lorenzo Monacelli^d, Giovanni Garberoglio^{a,e}, Nicola M. Pugno^{b,f}, Simone Taioli^{a,e,**}

^a*European Centre for Theoretical Studies in Nuclear Physics and Related Areas (ECT*), Fondazione Bruno Kessler, Trento, Italy*

^b*Laboratory of Bio-inspired, Bionic, Nano, Meta Materials & Mechanics, Department of Civil, Environmental and Mechanical Engineering, University of Trento, Italy*

^c*Dipartimento di Ingegneria, Unita' di Ricerca di Fisica non lineare e Modelli matematici, Università Campus Bio-Medico, Via Alvaro del Portillo 21, Roma, 00154 Italy*

^d*Università di Roma "La Sapienza", Rome, Italy*

^e*Trento Institute for Fundamental Physics and Applications (TIFPA-INFN), Trento, Italy*

^f*School of Engineering and Materials Science, Queen Mary University of London, UK*

1. Thermal expansion of MgH_2 nanoparticles

In the main text we have shown the percent bond length variation in the simplest cases in which the NPs present only two kind of bonds each. Indeed, the Mg_3H_6C NP present a planar structure in which the hydrogen atoms are single or double coordinated while in the Mg_4H_8A NP their are single or three coordinated. In Fig. 1 we show the same analysis in the case of more heterogeneous bond distribution for the NPs that represent local minimum of the potential energy. We fitted as in the main text the percentage variation of the bond length with the temperature using linear relations, finding the general trend of a decrease in the bond length of single coordinated hydrogen atoms, a stable bond length for double coordinated and an increased bond length for multicoordinated hydrogen atoms.

2. Frontiers orbitals of MgH_2 nanoparticles

In Figs. 2 and 3 we show the frontiers orbitals (HOMO and LUMO) calculated at DFT level for MgH_2 nanoparticles.

*Corresponding author

**Corresponding author

Email address: taioli@ectstar.eu (Simone Taioli)

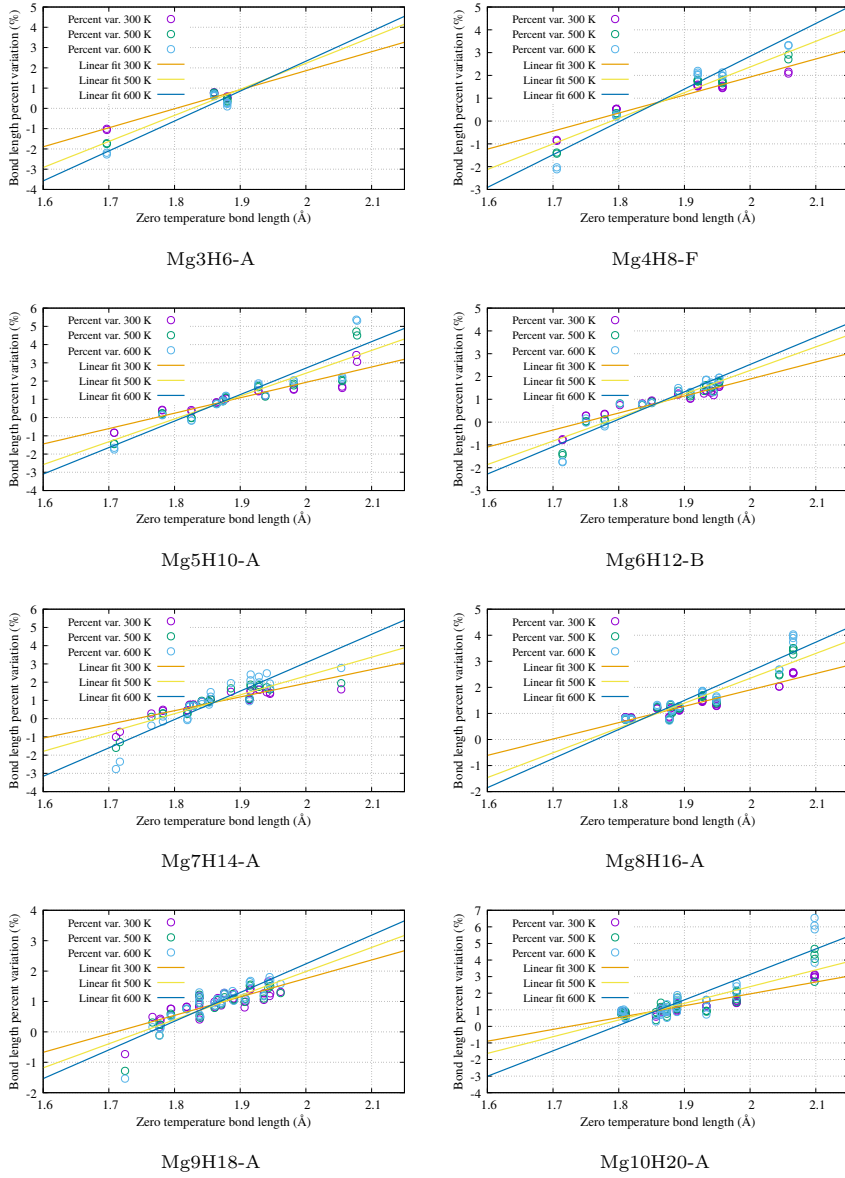


Figure 1: Percent bond length variation as function of temperature for MgH₂ nanoparticles. The graphs are reported for the structures with the lowest energy at fixed n .

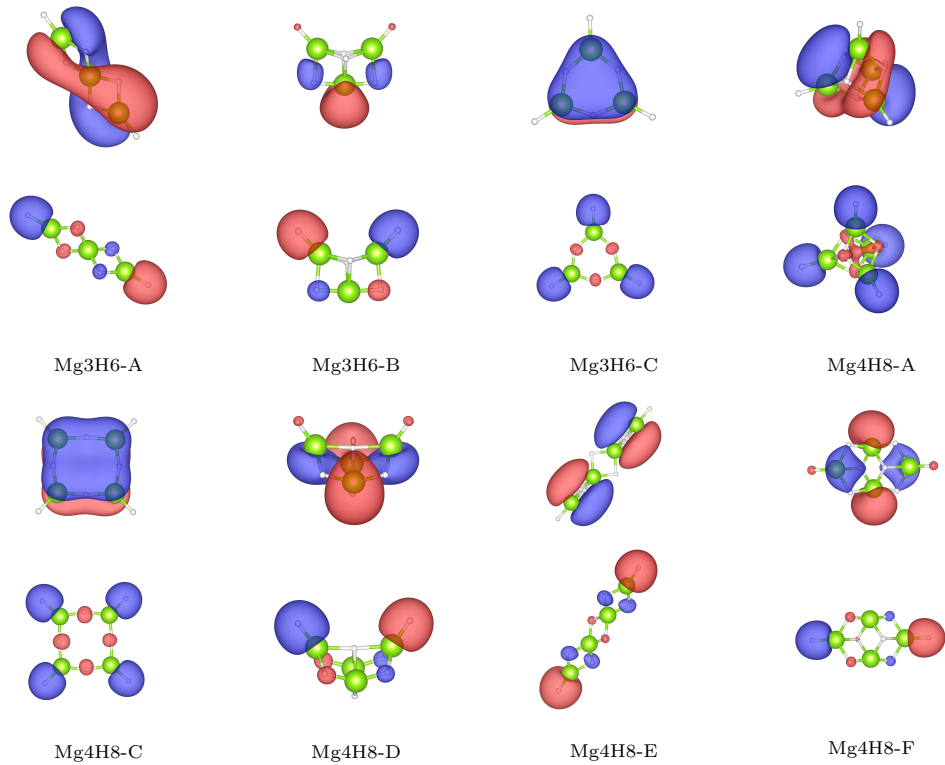


Figure 2: Frontiers orbitals (HOMO and LUMO) of MgH_2 nanoparticles. HOMO and LUMO are represented in the bottom and top panel, respectively, for each nanoparticle.

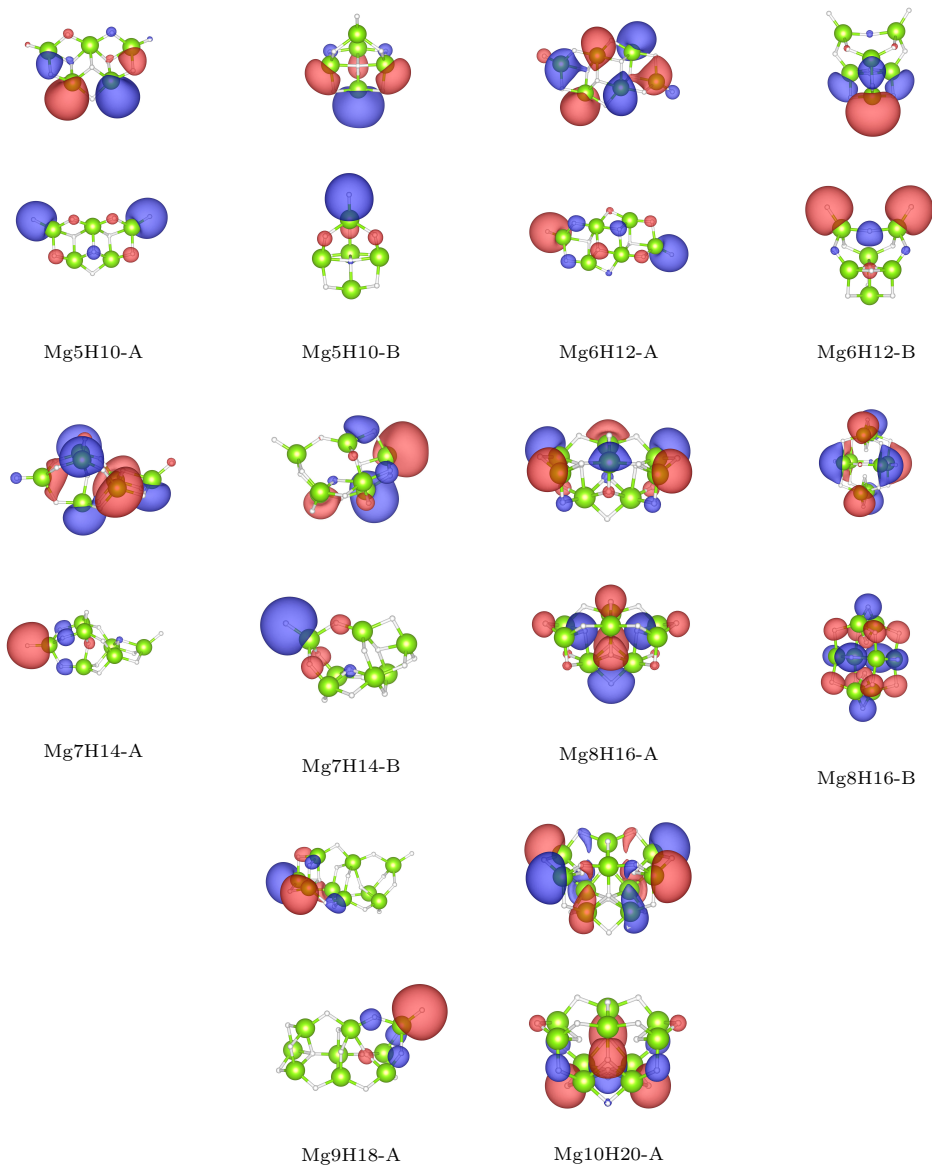


Figure 3: Frontiers orbitals (HOMO and LUMO) of MgH_2 nanoparticles. HOMO and LUMO are represented in the bottom and top panel, respectively, for each nanoparticle.

3. The partition function of molecular hydrogen

In the case of two H atoms the partition function reads:

$$q(T) = \frac{1}{2!} \sum_{\sigma} \int d^3R \langle \mathbf{R} | e^{-\beta \mathcal{H}} \mathbf{P}_{\sigma} | \mathbf{R} \rangle, \quad (1)$$

where $\mathcal{H} = K + V(\mathbf{R})$ is the Hamiltonian, written in relative coordinates \mathbf{R} of the two H isotopes of reduced mass μ as the sum of the kinetic energy $K = -\frac{\hbar^2}{2\mu} \frac{\partial^2}{\partial^2 R} + \frac{\hat{\mathbf{L}}^2}{2\mu r^2}$ ($\hat{\mathbf{L}}^2 = \hbar^2 L(L+1)$) and of the interatomic potential $V(\mathbf{R})$, and P_{σ} is the permutation operator, multiplied by the sign \pm for even or odd permutations of identical fermionic isotopes. The sum runs over all permutations σ of two atoms for identical particles, while $P_{\sigma} = 1$ for distinguishable particles. The eigenvalues $E_{L,n}$ of \mathcal{H} are labelled by the quantum numbers L , identifying the angular momentum, and n , identifying the energy level. States with angular momentum L are $(2L+1)$ degenerate. The range of the investigated temperatures is such that the H_2 molecule cannot dissociate, hence only bound states will be considered.

Additionally, the action of the permutation operator P_{12} that exchanges two particles depends on the parity $(-1)^L$. Hence in the case of identical bosons (H_2) only even angular momenta contribute to the partition function, whereas the opposite applies in the case of fermions.

3.1. SSCHA convergence

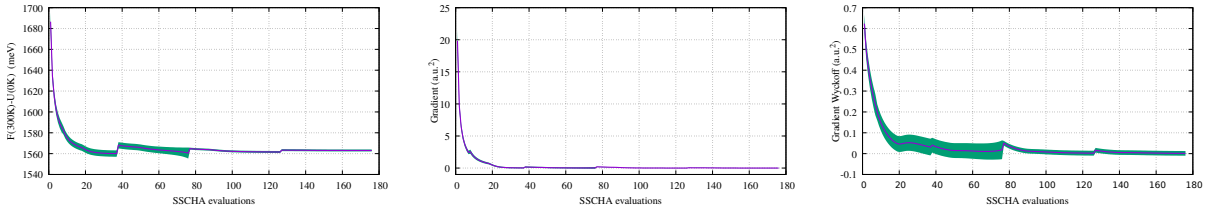


Figure 4: SSCHA free energy relative to $U(0K)$ (left panel), modulus of the free-energy gradient with respect to the dynamical matrix (middle panel) and modulus of the free-energy gradient with respect to the Wyckoff positions (right panel). The stochastic error is represented by a green band.

SSCHA proceeds through a series of repeated evaluation steps, the first being the generation of the stochastic population and the calculation of the energy and forces for each element of the population, the second being the minimization of the free energy using a reweighting procedure. The resampling is performed when the stochastic population due to the reweighting procedure is no more representative of the starting one.

In Fig. 4 we plot the convergence of the FHE (left panel), of the modulus of the free-energy gradient with respect to the dynamical matrix (middle panel), and of the modulus of the free-energy gradient with respect to the Wyckoff positions (right panel) upon application of the SSCHA method to the Mg_4H_8 NP at 300 K.

The first three minimizations up to ≈ 80 SSCHA evaluations correspond to stochastic populations of 10^3 elements each, the last two instead, where the stochastic error (green band in Fig. 4) decreases, correspond to populations of 10^4 elements each.